Continuous EEG Classification for Motor Imagery Interfaces Using Riemannian Alignment

Vladimir Antipov
Research Institute of Applied Artificial Intelligence and Digital Solutions
Plekhanov Russian University of Economics
Moscow, Russia
vantipovm@gmail.com

Susanna Gordleeva
Lobachevsky State University of Nizhny Novgorod
Nizhny Novgorod, Russia
gordleeva@ibbm.unn.ru

2026 10th Scientific School Dynamics of Complex Networks and their Applications (DCNA) | 979-8-3195-2599-4/26/$31.00 ©2026 IEEE | DOI: 10.1109/DCNA72004.2026.11733437

***Abstract*—This study addresses the adaptation of classification methods for multimodal bioelectrical signals to streaming processing, with evaluation on EEG recordings obtained during motor imagery. A processing module was implemented to coordinate continuous preprocessing, window formation, calibration and prediction with the events of the experimental protocol. Signal segments were represented by regularised covariance matrices, aligned using parallel transport on the manifold of symmetric positive definite matrices and classified using a support vector machine. Incremental updating of the reference statistics allowed adaptation to the current session, while asynchronous execution separated model operations from data acquisition. Recorded sessions were replayed through the same processing sequence used for incoming streams. In leave-one-subject-out validation on ten participants selected for the highest within-subject separability, window-level accuracy reached 0.68 ± 0.07. Majority voting within trials increased accuracy to 0.78 ± 0.09 and the F_1 score to 0.81 ± 0.06. Analysis windows were advanced at a configured interval of 0.5 s. These results support the proposed organisation of streaming classification and demonstrate the benefit of temporal aggregation within the evaluated subgroup.**

***Index Terms*—bioelectrical signals, streaming processing, EEG, motor imagery, brain-computer interface, Riemannian geometry**

I. Introduction

Restoration of motor function after neurological injury is a major objective of neurorehabilitation, motivating the development of technologies that engage brain activity in the rehabilitation process [1], [2]. Among these technologies, systems based on motor imagery provide a means of involving motor networks even when the ability to perform voluntary movements is impaired [3], [4]. The electrical activity accompanying imagined movements can be recorded using electroencephalography (EEG) and analysed to identify patterns associated with the intended action, such as event-related changes of sensorimotor rhythms revealed by time-frequency analysis [5]. This principle underlies brain-computer interfaces (BCIs), in which recognition of these patterns is used to control external devices and provide feedback to the user [6]–[8]. The practical implementation of such feedback requires the recorded activity to be processed continuously, so that the response of the system remains temporally related to the ongoing task, since the properties of feedback can themselves affect the brain state of the user [9].

This requirement brings the organisation of signal processing into direct connection with the intended application. Classification methods evaluated on complete recordings provide an estimate of how reliably the target states can be distinguished, but their use during an ongoing session also depends on how data acquisition, preprocessing and prediction are coordinated [6]. As samples arrive sequentially, each decision must rely on the available signal history, while filtering and feature extraction must preserve continuity across successive analysis windows. When several bioelectrical modalities are considered jointly, this processing sequence must also maintain their temporal correspondence. Adaptation of classification methods to streaming operation therefore requires a consistent organisation of the entire sequence through which incoming signals are transformed into feedback.

The continuity of this sequence must be maintained despite variability in the signals themselves. Differences between subjects and recording sessions can alter the statistical characteristics of EEG and reduce the reliability of models trained on other recordings [6]. Methods based on Riemannian geometry address this problem by representing signal segments as covariance matrices and aligning their distributions across recordings [10]–[12]. Their application to a continuous stream requires the reference statistics used for alignment to be estimated from the data available during the session. Calibration and subsequent updates must consequently be integrated with ongoing classification, allowing adaptation to proceed as new observations become available.

In this study, we address the adaptation of classification methods for multimodal bioelectrical signals to streaming processing. We present a processing module in which continuous preprocessing, window formation and model adaptation are coordinated with the events of the experimental protocol. The proposed organisation is evaluated on EEG recordings obtained during motor imagery, using a common processing sequence for recorded data replay and incoming streams.

Acknowledgments. The work was funded by the Russian Science Foundation (Grant No. 25-69-00047, https://rscf.ru/project/25-69-00047/).

Authorized licensed use limited to: Kant Baltic Federal Univ. Downloaded on October 23,2026 at 15:21:42 UTC from IEEE Xplore. Restrictions apply.

II. Methods

A. Data Acquisition and Experimental Protocol

The streaming processing approach was evaluated using EEG recordings obtained during a motor imagery task. The experimental protocol included oculomotor calibration, background recording, adaptation and inference periods. These periods provided the data required to initialise the preprocessing stages, estimate the characteristics of the current session and classify the activity recorded during task performance. Transitions between experimental phases were identified by markers generated by the stimulus program.

The module received data through the Lab Streaming Layer, using separate inlets for the EEG and marker streams. The EEG stream contained 21 channels sampled at 250 Hz. Incoming samples were associated with the corresponding experimental phase, allowing their subsequent use for calibration, adaptation or classification to be determined by the protocol.

B. Organisation of Streaming Processing

The processing module was organised around the continuous transformation of incoming samples into classification results (Fig. 1). Signal acquisition, preprocessing and window formation were coordinated with the experimental events, while model fitting and prediction were executed asynchronously. This organisation allowed computationally demanding operations to be submitted without requiring the acquisition loop to wait for their completion.

The correspondence between experimental phases and processing operations was specified by a finite state machine described in a configuration file. Each state defined the group to which the incoming samples were assigned, their class label and the operations initiated on entry, on exit or during a transition. The available operations comprised data collection, initial fitting, incremental updating and prediction. Where required, an operation could be delayed by a specified interval measured in stream time. The same processing stages could therefore be used at different points in the protocol, with their execution determined by the current experimental state.

C. Continuous Preprocessing

Samples were received in chunks and processed sequentially. Each sample was re-referenced to the configured reference electrode, converted from microvolts to volts and restricted to the 18 channels used for classification. The selected signals were then filtered between 4 and 40 Hz using a fourth-order Butterworth band-pass filter implemented in second-order-section form.

To support continuous processing, the internal filter state was retained between successive samples. The output consequently depended on the preceding signal history without requiring access to future observations. For the same initial conditions, this procedure corresponds to forward filtering of the continuous signal. Preserving the filter state also avoided introducing a new filtering boundary at each analysis window.

D. Formation of Analysis Windows

The preprocessed samples were accumulated in buffers associated with the data groups defined by the experimental protocol. Separate groups were used for oculomotor calibration, background recording, adaptation and inference. Buffers were segmented when the collecting group changed, so that windows were formed within the corresponding data segment.

A common window length of 750 samples, corresponding to 3 s, was used throughout the processing sequence. For inference, the window was advanced by 125 samples, providing a nominal prediction interval of 0.5 s once sufficient data had accumulated. For fitting and incremental updating, the step was equal to the window length. The resulting non-overlapping windows avoided repeated inclusion of the same samples within an individual fitting or updating sequence.

Each window was stored together with its boundary timestamps, session identifier, state visit index and sample labels. This representation preserved the relationship between the signal segment and the experimental conditions under which it was recorded. It also provided a common input format for fitting, adaptation and prediction.

E. Feature Extraction and Classification

Ocular artefacts were removed using independent component analysis [13]. The decomposition was fitted on the oculomotor calibration segment, and components associated with vertical and horizontal eye movements were identified automatically and excluded during signal reconstruction [14], [15]. A spatial whitening transform estimated from the background recording was subsequently applied to normalise the covariance structure of the current session.

To incorporate temporal information into the covariance representation, the whitened signals were augmented with delayed copies using an embedding order of four and a lag of eight samples. This transformation increased the signal dimension from 18 to 72. Each augmented window was represented by a covariance matrix estimated using oracle approximating shrinkage (OAS), which regularises covariance estimation when the number of observations is limited relative to the signal dimension [16]. The estimator has the form

$$\widehat{\Sigma} = (1-\rho)S + \rho\frac{\operatorname{tr}(S)}{p}I_p, \tag{1}$$

where S is the empirical covariance matrix, p is the signal dimension, I_p is the identity matrix and ρ is the shrinkage coefficient estimated by OAS.

The covariance matrices were aligned using parallel transport on the manifold of symmetric positive definite matrices [11], [12]. Spatial feature extraction was based on common spatial patterns, which identify projections informative for distinguishing the target classes [17], [18]. The implemented pipeline used a Riemannian formulation with ten components. The resulting features were passed to a support vector machine with a radial basis function kernel, which returned a predicted class and an associated confidence value.

Authorized licensed use limited to: Kant Baltic Federal Univ. Downloaded on October 23,2026 at 15:21:42 UTC from IEEE Xplore. Restrictions apply.

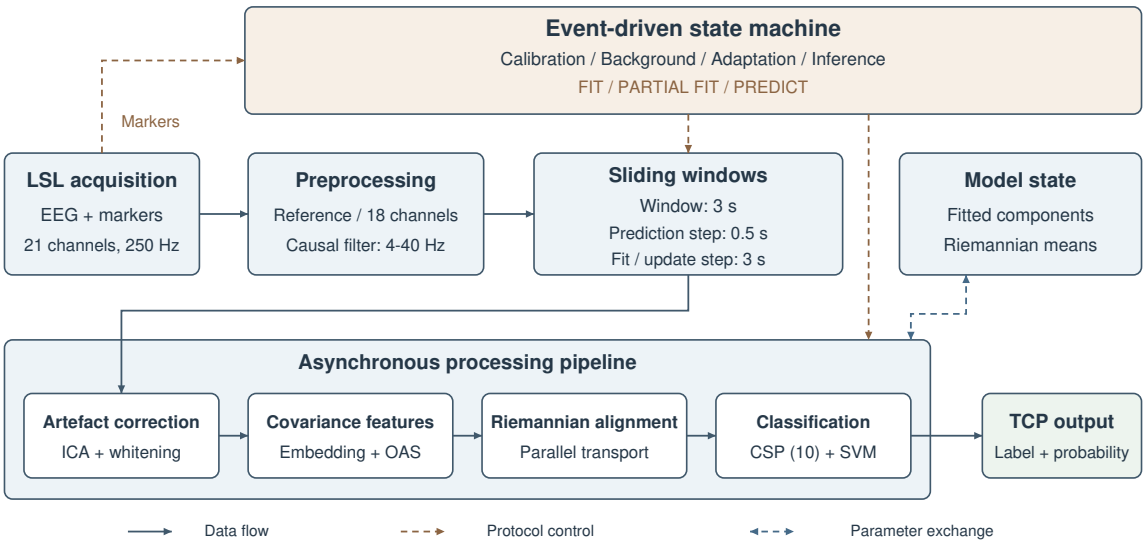


Fig. 1. Functional organisation of the streaming processing module. The data path (solid arrows) runs from the Lab Streaming Layer inlets through per-sample preprocessing and the sliding-window buffer to the asynchronous worker pool and the TCP output. The event-driven state machine (dashed arrows) does not touch the data itself: it decides, for every experimental phase, which logical group the incoming samples belong to, with which step the buffer is scanned, and which of the operations FIT, PARTIAL FIT or PREDICT is applied to the resulting windows. Components fitted or updated inside the worker pool are returned to the component store and reused by subsequent windows.

F. Calibration and Incremental Adaptation

Fitting was distributed across the experimental phases according to the data required by each processing stage. For components requiring calibration, a fitting operation passed the selected windows through the available transformations and estimated the parameters of the next unfitted stage. Previously trained components were loaded at initialisation, while session-specific transformations were fitted from the corresponding calibration segments. Prediction required all necessary components to be available; otherwise, the missing components were reported and processing continued with subsequent data.

Adaptation to the current subject was performed at the covariance alignment stage. This stage maintained a subject-specific Riemannian mean, a global reference mean and the numbers of windows supporting these estimates. When new adaptation windows became available, the means were updated using weighted Riemannian averaging of the previous estimates and the newly accepted covariance matrices. The accumulated information was therefore represented by the current means and their weights, avoiding repeated processing of the complete session history.

The contribution of an individual subject to the global reference was limited by a cap on the number of accepted windows. This restriction reduced the influence of a single session on the reference population. Alignment and subsequent prediction were performed only after at least five windows had contributed to the subject-specific mean. Before this condition was met, prediction for the corresponding window was skipped.

G. Asynchronous Execution and Feedback Output

Fitting, incremental updating and prediction were submitted to a pool of worker processes. Completed operations returned their results through callbacks, and fitted or updated components were stored for subsequent processing. This separation allowed signal acquisition and handling of experimental events to continue while the workers processed previously formed windows.

Classification results were placed in an output queue and transmitted by a separate process over a TCP connection. Each message contained the predicted label, its probability estimate, the window processing time and the associated metadata. The stimulus program could then use these messages to generate feedback linked to the classified signal segment.

H. Evaluation on Recorded Data

Recorded sessions stored in XDF format were replayed through the same state machine, preprocessing stages and windowing procedure used for incoming streams. Samples and markers were supplied in their recorded temporal order, and the marker sequence was checked against the selected protocol configuration before evaluation. This procedure preserved a common definition of the processing operations and experimental phases across recorded data replay and streaming acquisition.

Classification performance was assessed using leave-one-subject-out validation on ten subjects selected for the highest within-subject separability. In each fold, the pipeline was trained on the other subjects and adapted using a calibration subset from the held-out session. Performance was evaluated for individual windows and for complete trials, with trial

Authorized licensed use limited to: Kant Baltic Federal Univ. Downloaded on October 23,2026 at 15:21:42 UTC from IEEE Xplore. Restrictions apply.

predictions obtained by majority voting over their window predictions. Accuracy, precision, recall and F_1 score were summarised across subjects.

A separate within-subject reference analysis used nearest-neighbour classification based on Riemannian distances between covariance matrices in 22 subjects. Windows belonging to the same trial as the evaluated window were excluded from its neighbourhood. This analysis provided a reference for within-subject discrimination under a different training scheme.

III. Results

Evaluation on recorded motor imagery sessions showed that classification performance depended on whether decisions were considered at the level of individual windows or complete trials. In the leave-one-subject-out analysis of ten participants selected for the highest within-subject separability, classification of individual 3-second windows yielded an accuracy of 0.68 ± 0.07. Precision reached 0.84 ± 0.09, whereas recall was 0.48 ± 0.22, resulting in an F_1 score of 0.58 ± 0.17. All values are reported as the mean and standard deviation across participants. The difference between precision and recall indicates that the window-level operating point favoured the reliability of positive predictions while leaving a substantial proportion of the target events undetected.

Aggregation of window predictions within each trial improved the resulting classification. Majority voting increased accuracy to 0.78 ± 0.09 and recall to 0.89 ± 0.09, with an F_1 score of 0.81 ± 0.06. The increase of approximately ten percentage points in accuracy shows that combining decisions over the trial provided a more reliable estimate of the target state than classification of an individual window. This improvement is consistent with the temporal variability of the evidence available within a trial, where individual segments may differ in how clearly they represent the classified activity. The results therefore support the use of accumulated window predictions when a decision characterising the complete trial is required.

A separate within-subject analysis provided a reference for the discrimination achievable from covariance representations. Nearest-neighbour classification based on Riemannian distances, with windows from the evaluated trial excluded from the neighbourhood, reached an accuracy of 0.80 ± 0.09 and an F_1 score of 0.80 ± 0.10 across 22 participants. These values were numerically close to the trial-level results of the streaming pipeline. However, the analyses differed in their participant sets, training procedures and prediction units, so this comparison does not establish equivalent performance or isolate the contribution of covariance alignment.

During recorded data replay, predictions were generated from overlapping windows with a configured step of 0.5 s after the initial window had accumulated and the required processing components were available. This organisation supported repeated assessment of the incoming activity and subsequent aggregation of decisions within a trial. The interval describes the temporal spacing of analysis windows; the present evaluation does not establish the end-to-end latency of feedback delivery during live operation.

Conclusion

This study presents an approach to adapting classification methods for multimodal bioelectrical signals to continuous data processing. The implemented module coordinates preprocessing, analysis window formation and model updates with the experimental protocol, providing a common processing sequence for incoming streams and recorded data replay. Incremental estimation of the Riemannian reference means supports adaptation of covariance representations to the current session, while asynchronous execution allows acquisition to continue during fitting and prediction. Subsequent work should assess performance in a broader participant population, quantify latency during live operation and evaluate joint processing of multiple bioelectrical modalities, as well as their combination with hemodynamic signals such as functional near-infrared spectroscopy [19].

References

[1] V. Khorev, S. Kurkin, A. Badarin, V. Antipov, E. Pitsik, A. Andreev, V. Grubov, O. Drapkina, A. Kiselev, and A. Hramov, "Review on the use of brain computer interface rehabilitation methods for treating mental and neurological conditions," *Journal of Integrative Neuroscience*, vol. 23, no. 7, p. 125, 2024.

[2] V. Khorev, A. Kiselev, A. Badarin, V. Antipov, O. Drapkina, S. Kurkin, and A. Hramov, "Review on the use of AI-based methods and tools for treating mental conditions and mental rehabilitation," *The European Physical Journal Special Topics*, vol. 234, no. 15, pp. 4139–4158, 2025.

[3] A. E. Hramov, V. A. Maksimenko, and A. N. Pisarchik, "Physical principles of brain–computer interfaces and their applications for rehabilitation, robotics and control of human brain states," *Physics Reports*, vol. 918, pp. 1–133, 2021.

[4] V. Antipov, S. Kurkin, and S. Gordleeva, "Higher-order triadic interactions in the eeg sensorimotor network during motor imagery," *The European Physical Journal Special Topics*, pp. 1–9, 2026.

[5] L. Kralj, S. Kurkin, H. Lenasi, A. Pavlov, A. Stožer, A. E. Hramov, M. Perc, and M. Gosak, "Wavelet analysis in biomedical research: A versatile tool for multiscale signal characterization and functional connectivity analysis," *Physics of Life Reviews*, vol. 59, pp. 19–47, 2026.

[6] F. Lotte, L. Bougrain, A. Cichocki, M. Clerc, M. Congedo, A. Rakotomamonjy, and F. Yger, "A review of classification algorithms for eeg-based brain–computer interfaces: a 10 year update," *Journal of neural engineering*, vol. 15, no. 3, p. 031005, 2018.

[7] V. Antipov, "Upper limb exoskeleton for neurorehabilitation with control via brain-computer interface," in *2022 6th Scientific School Dynamics of Complex Networks and their Applications (DCNA)*. IEEE, 2022, pp. 21–23.

[8] N. A. Grigorev, A. O. Savosenkov, M. V. Lukoyanov, A. Udoratina, N. N. Shusharina, A. Y. Kaplan, A. E. Hramov, V. B. Kazantsev, and S. Gordleeva, "A BCI-based vibrotactile neurofeedback training improves motor cortical excitability during motor imagery," *IEEE Transactions on Neural Systems and Rehabilitation Engineering*, vol. 29, pp. 1583–1592, 2021.

[9] V. A. Maksimenko, A. E. Hramov, V. V. Grubov, V. O. Nedaivozov, V. V. Makarov, and A. N. Pisarchik, "Nonlinear effect of biological feedback on brain attentional state," *Nonlinear Dynamics*, vol. 95, no. 3, pp. 1923–1939, 2019.

[10] A. Barachant, S. Bonnet, M. Congedo, and C. Jutten, "Multiclass brain–computer interface classification by riemannian geometry," *IEEE Transactions on Biomedical Engineering*, vol. 59, no. 4, pp. 920–928, 2011.

[11] P. Zanini, M. Congedo, C. Jutten, S. Said, and Y. Berthoumieu, "Transfer learning: A riemannian geometry framework with applications to brain–computer interfaces," *IEEE Transactions on Biomedical Engineering*, vol. 65, no. 5, pp. 1107–1116, 2017.

Authorized licensed use limited to: Kant Baltic Federal Univ. Downloaded on October 23,2026 at 15:21:42 UTC from IEEE Xplore. Restrictions apply.

[12] O. Yair, M. Ben-Chen, and R. Talmon, "Parallel transport on the cone manifold of spd matrices for domain adaptation," *IEEE Transactions on Signal Processing*, vol. 67, no. 7, pp. 1797–1811, 2019.
[13] E. Oja and A. Hyvarinen, "Independent component analysis: algorithms and applications," *Neural networks*, vol. 13, no. 4-5, pp. 411–430, 2000.
[14] V. Antipov and A. Badarin, "Development of an algorithm for detecting saccadic eye movements based on model approximation," *Bulletin of the Russian Academy of Sciences: Physics*, vol. 89, no. 3, pp. 476–481, 2025.
[15] V. Antipov, "Comparison of wearable video-based eye tracking and eog for oculomotor activity detection in specific research tasks," in *2024 8th Scientific School Dynamics of Complex Networks and their Applications (DCNA)*. IEEE, 2024, pp. 13–15.
[16] Y. Chen, A. Wiesel, Y. C. Eldar, and A. O. Hero, "Shrinkage algorithms for mmse covariance estimation," *IEEE transactions on signal processing*, vol. 58, no. 10, pp. 5016–5029, 2010.
[17] H. Ramoser, J. Muller-Gerking, and G. Pfurtscheller, "Optimal spatial filtering of single trial eeg during imagined hand movement," *IEEE transactions on rehabilitation engineering*, vol. 8, no. 4, pp. 441–446, 2000.
[18] B. Blankertz, R. Tomioka, S. Lemm, M. Kawanabe, and K.-R. Muller, "Optimizing spatial filters for robust eeg single-trial analysis," *IEEE Signal processing magazine*, vol. 25, no. 1, pp. 41–56, 2008.
[19] A. E. Hramov, V. Grubov, A. Badarin, V. A. Maksimenko, and A. N. Pisarchik, "Functional near-infrared spectroscopy for the classification of motor-related brain activity on the sensor-level," *Sensors*, vol. 20, no. 8, p. 2362, 2020.

Authorized licensed use limited to: Kant Baltic Federal Univ. Downloaded on October 23,2026 at 15:21:42 UTC from IEEE Xplore. Restrictions apply.